

**MODIS Team Member - Semi-Annual Report
Marine Optical Characterizations
December 1995**

**Dennis K Clark
NOAA/NESDIS**

SUMMARY



The past team's emphasis during this reporting period has been in the areas of assembling the operational Marine Optical Buoy (MOBY), testing and developing bio-optical instrumentation and measuring techniques, collecting turbid and clear water data for ocean color satellite algorithm development, and data processing. During this reporting period, the Team conducted four field experiments, acquiring measurements which cover water types from very turbid to very clear, and produced comprehensive bio-optical data sets. The operations schedule for the field experiments is shown in Figure 1. These data sets are being analyzed to evaluate the bio-optical protocols (i.e. remote sensing reflectance, diffuse attenuation coefficients, and water-leaving radiances) and the effects of instrument self-shading. Technical memoranda are being written that address the remote sensing reflectance and the particle absorption protocols.

The MOBY mooring off Lanai was replaced. A sun photometer system (CIMEL) was installed at a remote site on the northwest coast of Lanai, approximately seven miles from the MOBY mooring. The CIMEL site construction and installation was done in support of Brent Holman and Robert Frouin (NASA GSFC and Headquarters, respectively).

MOCE/TURBID-3 AND MOCE/TURBID-5 EXPERIMENTS

A series of measurements was conducted at Mill Creek (a northwestern Chesapeake Bay tributary), from July 24 to August 4, and from September 21 to October 13, to verify the "remote sensing reflectance" protocols and examine the polarization effects, which are not presently considered by the protocol. Sky, water, and plaque polarization were measured using a linear polarizer and a photodiode at zenith angle of 20 degrees and azimuth angles of 90, 95, 100, 105, 120, and 135 degrees relative to the sun (Figure 2). To provide data for the atmospheric correction algorithm visible and N IR casts were performed with 1 mm bare fiber and the Collector Head from the surface down to a depth of 120 cm in very turbid waters (Figure 3). Coincident water samples for phytoplankton pigment concentration, total suspended material, particulate and detrital absorption, and dissolved organic matter analyses were collected. Breakdown of water samples collected is as follows:

**Turbid-3: 30 HPLC samples
18 Fluorescence samples
11 Particulate/Detrital absorption samples
8 Total suspended material samples**

**Turbid-5: 52 HPLC samples
51 Particulate/Detrital absorption samples
16 Total suspended material samples
24 Dissolved organic matter samples**

The following personnel participated:

**NOAA - Dennis Clark, Yuntao Ge, Phil Hovey, Ed King, Eric Stengel,
Marilyn Yuen, Larisa Koval
CHORS - Chuck Trees**

MOBY-LIO/TURBID-4 EXPERIMENT

The MOCE team was in Hawaii, from August 15-30, to continue assembling the Marine Optical Buoy (MOBY) and to obtain additional turbid water data for ocean color satellite algorithm development. Radiance and irradiance data in the visible (380-730 nm) and near IR (560-1100 nm) regions were collected to quantify measurement fluctuations due to wave focusing and water molecule backscattering, instrument self-shading effects, and sky polarization effects. Turbid water profiles were obtained using both the Rainbow Spectrometer system and a turbid water profiling system (fluorescence, beam attenuation, and depth) to provide data for the atmospheric correction algorithm.

The following personnel participated:

**NOAA - Dennis Clark, Yuntao Ge, Phil Hovey, Ed King, Eric Stengel,
Marilyn Yuen, Larisa Koval
CHORS - Chuck Trees
MLML - Mark Yarbrough, Yong Sun Kim**

Wavelength calibration was carried out for both the NIR and Visible Rainbow Spectrometer systems using Krypton, Mercury, and Neon lamps. It was found that both systems have a linear wavelength-pixel relationship.

NIR system:

- o left channel: wavelength=1127.53-4.16867*pixel**
- o right channel: wavelength=38.6112+4.13781* pixel**

Visible system:

- o left channel: $\text{wavelength}=715.914-2.74262*\text{pixel}$
- o right channel: $\text{wavelength}=41.5030+2.73912*\text{pixel}$

The accuracy of this calibration was verified by using a He-Ne laser emitting at 543.5 nm and a photo-diode laser emitting at 670 nm.

Radiance calibration was carried out for both the NIR and Visible Rainbow Spectrometer systems using the Optronic 420M integrating sphere. The following configurations were calibrated:

- o 1 mm fiber with radiance collector head
- o 1 mm bare fiber
- o 1 mm bare fiber with a field-of-view limiter

Irradiance calibration was performed for both Rainbow Systems using the standard lamp GS922. System response for the NIR and Visible Rainbow Spectrometer Systems is illustrated in Figures 4 and 5. The long term stability of both Rainbow Systems was monitored using an RS-10 reference lamp. The following configurations were calibrated:

- o Irradiance head with 200 micron fiber
- o Radiance head with 200 micron fiber
- o 1 mm bare fiber

A submersible platform was built to hold the Sea-Tech transmissometer, Wet Labs fluorometer, and a depth transducer in order to provide high sensitivity bio-optics within the first several meters of water depth (Turbid Water Profiling System) (Figure 6). This new system was used with the Visible Rainbow system to obtain turbid water profile data.

A set of observations was performed in an effort to quantify the effects of sky polarization and self-shading. To simulate the self-shading of the in-water optical instruments, several disks of different diameter were used (Figure 7). The results are being evaluated.

Remote sensing reflectance was measured according to the SeaWiFS protocol and technique used by Ken Carder. The effect of solar zenith angle on the remote sensing reflectance is shown in Figure 8 and illustrates that the large errors exist due to polarization. Improvement in the protocol is being recommended based on these data.

MOBY-L11/TURBID-6 EXPERIMENT

Ship time was from November 3-8. The following personnel were involved:

NOAA- Dennis Clark, Edward King, Edward Fisher, Yuntao Ge, Phil Hovey, Larisa Koval

**MLML- Mike Feinholz, Drew Gashler, Mark Yarbrough, Yong Sun Kim
University of Miami -Al Chapin, Yi Liu, Karl Moor, Joe Ritter
Mooring Systems, Inc. - Peter Clay, Don Dooner
University of Hawaii - Mike Ondrusek**

Further work was accomplished on mechanical and electrical assemblies on the MOBY-2 buoy at the Sand Island facility in Honolulu. The buoy is mechanically complete. Work is nearing completion on the MOBY-2 controller hardware which involves relay boxes and power terminals for the instrument, communication, and battery charging system.

The refurbishment of recycled mooring components (surface float, glass balls, flounder plate, acoustic release) was completed. Peter Clay from Mooring Systems, Inc., who manufactured the MOBY-2 surface flotation and the deep sea mooring system, joined NOAA and Moss Landing Marine Laboratories personnel in Hawaii for the MOBY-L11 mooring replacement. The deep sea mooring is scheduled for replacement at 12 month intervals, but due to the pressure of work on MOS-2, the mooring was delayed from August to November. Recovery of the mooring and deployment of the replacement went well (Figure 9). This recovered mooring was in better shape than the previous mooring with the exception of the shackle attached to the surface float bail. The nut and pin threads on this shackle were corroded to the point of being useless, the cotter pin was basically all that was holding the pin in the shackle.

During the shipboard cruise, a full set of measurements of clear water was performed, including remote-sensing reflectance, water leaving radiance, attenuation coefficients, self-shading effects, pigment concentration, fluorescence, polarization effects, and transmission coefficients. AC-9 data were collected in conjunction with the Turbid Water Profiling System. This was the first cruise in which the instrument did not develop noise problems, and the air calibration remained stable for the duration of the cruise and consistent with the lab values.

A system for suspending surfaces with different reflectance characteristics was constructed to be used as a underwater filming target. (Figure 10). Underwater video documentation was acquired for the different reflectance targets at different near-surface depths. The imagery will assist in the interpretation of the wave focusing effects of the nadir upwelled radiances,

Wavelength calibration was carried out for both the NIR and Visible Rainbow Spectrometer systems using Neon and Mercury-Neon lamps. The calibrations demonstrated that both systems have a linear wavelength-pixel relationship. The long term stability of both Rainbow systems was monitored using an RS-10 reference lamp. The following configurations were calibrated:

- o Irradiance head with 200 micron fiber
- o Radiance head with 1 mm fiber

Radiance calibration was carried out for both NIR and Visible Rainbow Spectrometer systems using the Optronic 420M integrating sphere. The following configuration were calibrated:

- 01 mm bare fiber # 2
- 01 mm bare fiber # 3
- 01 mm bare fiber # 4
- 01 mm fiber # 2 with radiance collector head
- 01 mm fiber # 2 with old and new radiance collector heads
- 01 mm fiber # 3 and # 4 coupled together with and without gel

Irradiance calibration was performed for both Rainbow Spectrometer systems using the standard lamp (GS922). The following configurations were calibrated:

- 0200 micron fiber # 1 with old and new irradiance collector head
- 0200 micron fiber # 8 with old and new irradiance collector head

Sensitivity of the Rainbow Spectrometer System to polarization was tested using the Optronic 420M integrating sphere to generate non-polarized light. A Mellors Griot linear polarizer was put in front of the light collectors to allow only polarized light into the measurement system. Figure 11 shows the instrument setup and polarization sensitivity at several wavelengths for both Visible and NIR Spectrometer Systems. It is clear that the fiber has completely depolarized the light field that enters the spectrometer. No variation due to polarization was observed.

Upon arrival at the operations site, post-calibrations were performed, this round included the new UV Rainbow System. The immersion factor for the new irradiance collector was measured using the collimated source and filtered sea water. Another series of measurements was conducted at Snug Harbor, including self-shading test, Visible and NIR casts, and polarization characters of the water leaving radiance.

A sun photometer system (CIMEL), provided by Brent Holman (NASA GSFC), was installed at a remote site on the west northwest coast of Lanai near Pinacles Point (Figure 12). The site is approximately seven miles from the MOBY mooring and provides for unobstructed solar observations to the south and west. The mounting

platform was constructed during this deployment and erected with the instrumentation during the cruise. Robert Frouin from NASA Headquarters performed the instrument initialization and tests on November 11. The instrument was determined to be functioning and properly transmitting data via the GOES telemetry link at the site. I have informally agreed to provide operational support for this site.

MOCE INSTRUMENTATION

Instrumentation Hardware Status

As shown in Table 1, the majority of the MOCE instrumentation is fully functional. Exceptions to this are the MOS-2, Martec transmissometer, HHCRM, and NIST radiometer, which are in the testing and evaluation stage. The AC-9, VLST, scattering meter, photosynthetron, sky camera, air temperature and relative humidity sensors, towed paravane system, and diver calibration lamps, are either being modified or refurbished.

The two new Navy surplus mobile vans were shipped to Hawaii. These vans were converted into an optics calibration and optical/electronics assembly labs. During the October deployment the new vans were furnished, all light leakage was blocked and dust control systems installed. The labs were cleaned and all the optical calibration instruments and benches were installed.

Instrumentation Software Status

With the exception of MOS-2, all of the data acquisition software is fully functional (Table 2). No progress has been made on MOS-2 software since the last report. When the new spectrographs from American Holographic have been installed, the final stages of software testing will begin. The majority of the data processing routines are fully functional with modifications being implemented into AC-9 and HP spectrophotometer processing software. The scattering meter, particle counter, and sky camera processing software are still in development and testing phases.

MARINE OPTICAL BUOY

Software development

Updating window software from UIS windows to Xwindows version 11 (also called DEC windows) was completed. Three types of window software required modification: text, menu, and graphics. The text window is used to display data in a simple text form and includes scrolling. The menu window displays choices to control execution of a data acquisition (or any) program, for example, the graphics window plots data from instruments.

The reasons for this conversion are several: (1) to increase speed, (2) to make the software compatible with machines running Xwindows, (3) UIS is proprietary software of DEC and is not supported across other manufacturer's machines, (4) to allow Xwindows to be displayed on different machines that have an XI 1 server, and (5) UIS does not support colors, while Xwindows allows up to 256 colors to distinguish plotted data.

The UIS routines required driver software to emulate Xwindows which consume CPU time. An increased speed, by a factor of five, is realized for the next window. No change is observed in the menu window. The graph window, however, is slower by a factor between one and three. The major cause of this time consumption is that text rotation transposes a text image bit by bit. A second cause might be that Xwindows uses protocol language between the client and server so windows can be displayed across networked machines.

Low level Xwindows routines (XLIB) are used to replace the UIS routines. Although the details between XLIB and UIS routines differ somewhat, the basic graphic concepts are identical so the conversion was accomplished with minimum difficulty. The major difficulty was that Xwindows does not support text scaling and rotation.

Commercially available PC software is being evaluated for data acquisition and data processing capabilities. The software chosen includes LabView, HP VEE, HP BASIC, MATLAB and IDL. This is the first step towards moving data acquisition and data processing from the VAXstation to DOS machines to simplify our computer requirements.

Hardware development

MOS

All of the internal modification parts for MOS have been fabricated and anodized. Little more can be done in assembling MOS until the VS-10 spectrographs arrive from American Holographic. To determine the cause of delays in the delivery of that instrument, Dennis Clark, Mark Yarbrough, and Yuntao Ge traveled to the American Holographic facility near Boston in December. Delivery of the spectrographs was scheduled for the end of December 1995, but as of this writing we are still waiting for their delivery. The new design looks promising. The CCD mount required changes to allow rotational adjustability and to avoid additional disassembly of the CCD head which would have been necessary to mount the unit. Based upon the drawings obtained from American Holographic, MLML personnel proceeded with most of the remaining modifications to the two MOS units currently under construction. These modifications are for the power supplies, remaining

electronics mounts, and VS-10 interface. The remaining parts for the optical interface of the VS-10 to the MOS and parts for the VS-10 mount have been designed and are in fabrication.

MOBY PROTOTYPE

The MOBY test controller (previously deployed at the MOBY site) was recovered during the MOBY-L10 trip. The controller ran properly the entire time on its backup battery. It was impossible to contact the controller by cell phone because the modem had failed. Destructive testing of the controller and modem on Oahu isolated the problem to overheating of the modem. The temperatures inside the unshaded controller box can be in excess of 60°C which appears to be the temperature where the modems are damaged. In order to avoid this condition, the modems were heat sunk and the controller unit shaded. Shading reduced the controller temperature by about 20°C. Even though the modem appears to function well under these conditions, its use during midday hours will be avoided as an added precaution.

An attempt was made to redeploy the MOBY test controller at the Lanai site. This attempt was thwarted due to poor sea conditions and failure of the MOBY cell phone transceiver. The cell transceiver was damaged during reassembly of the controller. The cell transceiver was later repaired and the controller is functional. The MOBY test controller is currently on Maui island.

Some communications tests were performed from California with the unit on shore in Maui. This testing demonstrated that the MOBY files (250 kb) must be broken into smaller files for reliable transmission. Presently, 150 kb file transfers to the MOBY site in Hawaii and 30 kb file transfer to Moss Landing Marine Labs in California are possible. File transfers are limited by the length of the time the modems can stay connected. To eliminate the possibility of the MOBY controller receiving potentially system-crashing characters, the modems must be configured for a "high reliability only" mode of operation. This operating mode requires a minimum level of signal quality between the modems. The modems disconnect when signal quality drops to this base signal level. Signal degradation caused by the cell phone connection and the long distance connections requires shorter connection periods between the modems.

The solution is to support partial file transfers from MOBY. This change is currently implemented in the MOBY system. In the operational mode, the files will be dumped scan by scan from MOBY to the VAX machine at Snug Harbor and then sent via Internet from Hawaii to California. This will allow us to eliminate the poor quality long distance connection from the already marginal cell phone link to MOBY. It will also save money by eliminating the toll charge for the Hawaii to California transfer.

MOBY-2

The RSI fiber-optic collector heads, GFO fibers, and fiber feedthroughs were delivered to Hawaii in August. Some of the mechanical assembly tasks on MOBY-2 and MOBY-3 were completed during the MOBY-L10 trip. The new collector heads were fitted to the arms and the battery cables were assembled. The access hatches were added to the lower instrument bay, and the parts were made to adjust the position of the solar panels to fit the new electrical boxes. The electrical assembly of the solar panels was finished, and each unit has been load tested.

During the MOBY-L11 mooring replacement cruise, a fiber termination “pistoned”. General Fiber Optics is working on a new fiber connector design which doesn’t require epoxy. The new connector will not be available for at least three months. In the buoy, these fibers will not be subjected to tensions as great as those experienced during the vertical profiling. A set of fibers were pressure tested to 10 meters equivalent pressure for 24 hours in an attempt to check for gross flaws in the terminations. The presumption is that the pressure will cause the jacket length to shorten, in effect trying to push the fiber out of the termination. The terminations held and they didn’t leak. GFO is in the process of performing destructive testing on terminations made with the different epoxy types.

At the present, our greatest priority is to assemble a complete MOBY-2 mock-up test unit. This mock-up will be used at the Salinas Vertin Avenue facility to debug the TT7 microprocessor controller, hardware and software. That will include:

- o solar panel battery charging cycles
- o data acquisition scheduling
- o archiving MOCE-2 radiometric and ancillary data
- o data transmission via cellular modem
- o determining power budgets for all subsystems

DATA REDUCTION

MOCE-2

The reconstruction of MOCE-2 data sets is continuing. The VLST vertical data set is not finished because of the trouble with the depth register utility. A system of extracting the data through a series of hand operations using spreadsheets has been developed. This data set will be completed and checked. Scanning of MOCE-2 skycam data is completed. The movies and still pictures were created and digitized. A sample data file, in both jpeg and pict formats, for the digitized sky state photographs was submitted to NASA for evaluation. As of this time, NASA has not

provided information regarding which format would best integrate into their existing data base setup.

MOCE-3

The work is continuing on processing radiometric data from the MOCE-3 cruise. During the previous MOCE cruises, it became apparent that there was a problem matching processed spectra from the blue and red spectrographs where their wavelength ranges overlapped. The size and “direction” of this overlap offset changes between consecutive scan sets and throughout the cruise. Possible explanations for this discrepancy include:

- o Array temperature variations may affect system response.
- o Instrument temperature variations may affect dichroic transmission spectra.
- o Instrument temperature variations may affect dichroic wavelength response.
- o Pixel shifts from spectrographs may offset wavelengths.
- o Wavelength calibration may not match in overlap region.
- o System response may not be linear with integration time.
- o Integration times may not be exact.
- o Dark current may drift during the course of a scan set.
- o System and/or environmental noise may shift blue signal relative to red.
- o Data processing step(s) may create/increase the offset.
- o Surface wave focusing may not be being averaged out.

After conducting many exploratory tests on the data base, the preliminary conclusion is that the offsets are produced by a combination of inexact integration time and high environmental noise level. Integration time is selected from seven values (0.25, 0.5, 1,2,4,8, 16 sec) and is set by the SC controller. If one integration time is not exactly a factor of two different from the next time, system response (expressed in ADU counts per second) will not be exactly valid. This was found to be the case when a system response derived from a radiance calibration at 1/1 sec blue/red integration time was applied to a 1/0.5 sec radiance scan of the same source and the blue/red overlap did not exactly match (Figure 13). The photometries CCD controller in MOS-2 provides increased user control of integration time, so this contribution to the overlap problem may be solved on MOS-2.

In the 78 processed scan-sets from MOCE-3, there were 25 instances where the overlap offset relative to the signal at 609 nm was greater than 1/SNR from the blue array at 609 nm. Of the 25 cases, 6 had overlap offsets more than a few percent greater than the total blue and red environmental noise. This indicates that the size of the overlap offset is comparable to the environmental noise level (Table 3). Again, MOS-2 should solve this problem with increased SNR by lowering dark counts and allowing longer integration times. A test of this hypothesis would be to collect many

scans to average and reduce environmental noise, the size of the overlap offset should thus be reduced.

Alternatively, environmental noise due to periodic fluctuations of the underwater light field (caused by surface wave focusing) may be aliased by the integration times. Collecting more observations, either by increasing integration time per scan or by increasing the number of scans, should decrease this effect.

For the MOCE-3 experiments, the blue and red spectrographs were modified in an attempt to account for drifting dark count levels during a scan-set by “masking” a series of pixels at the far end of each diode array. The masked pixels’ level during a “lite” scan can be compared to levels during a “dark” scan and any offset applied to all unmasked “lite” pixel levels. We modified the dark-adjust software to process masked pixel information. Table 4 shows these offsets for one MOCE-3 station. Masked pixel offsets during both calibration and field scans appeared random, and processing with masked pixel offsets in system response and field scans did not reduce the overlap offset (Tables 3, 4). The temperature of the cooled array seemed not to correlate with the size or direction of the overlap offset. Masked pixel offsets also showed no relationship to array temperatures. It is not yet clear if internal instrument temperature is related to these offsets (via response of the dichroic mirror).

Occasionally, the output from the spectrographs is randomly shifted by +/- 1 pixel. The source of this problem is in the SC controller. This random shift could affect the wavelength fit in the overlap but probably not affect the intensity offset. The new spectrographs in MOS-2 should eliminate this problem. Wavelength calibration of blue and red arrays in the overlap region may not exactly match because different equations are used for the two spectrographs to fit the line source calibration points.

Based on the preliminary conclusion that the overlap offset was “in the noise,” field data were reprocessed by subtracting the offset at 609 nm from the blue array data before deriving attenuation coefficients and water-leaving radiances. System response was derived without processing masked-pixel offsets. This effectively reduced the spiking when scans were ratioed to calculate attenuation coefficients. The magnitude of the offsets for each scan set is given in Table 3.

New beta corrections for spectral photometric particle absorption measurements were developed and applied to the MOCE-2 and MOCE-3 data. A report discussing the protocols for the beta determinations is in preparation.

The MOCE-3 VLST vertical and along track data set is near completion.

A full MOBY synthetic data set was prepared for SeaWiFS Data Processing System. Daily files were created to simulate daily acquisition of MOBY data.

A database program was designed and completed to manage the MOCE Team's photographic database.

A brief summary for each MOCE-3 data set that has been transferred to NASA follows:

o Radiometric Data

- Marine Optical System (MOS) -14 data files transferred
- Marine Environmental Radiometer (MER) -14 data files transferred

0 CTD Data -19 data files transferred

0 Meteorological Data -3 data files transferred

0 Navigation Data -1 data file transferred

0 Flowmeter Data -16 data files transferred

o Absorption Data:

- Profile Particulate -19 data files transferred
- Along track Particulate -12 data files transferred
- Profile Detrital -18 data files transferred
- Along track Detrital -10 data files transferred

DOCUMENTATION

Moss Landing Marine Laboratories personnel have prepared two technical memoranda:

Feinholz, M.E. (1995) File structure for Marine Optical Buoy and Marine Optics System data. MLML Technical Memorandum 95-2.25 pp.

Gashler, J.A., W.W. Broenkow, and M. E. Feinholz (1 995) MOBY pressure and inclination 26 February to 22 March 1994. MLML Technical Memorandum 95-3, 15 pp.

SeaWiFS REVIEW

SeaWiFS prelaunch review took place at NASA/GSFC, August 8-10, 1995. D. Clark presented progress made by the MOCE team since last December, and Dr. W. Broenkow from Moss Landing Marine Laboratories presented the status of the

upgraded MOBY.

SUPPORTING GRANTS AND INTERAGENCY ACTIONS

The Research and Data Systems (RDS) Corporation science support contract has been completed.

A one year site support contract to the University of Hawaii, Marine Operations has been completed.

Funds were transferred to NSF UNOLS for University of Hawaii ship time support for MOBY.

The San Diego State University, CHORS grant extension was completed.

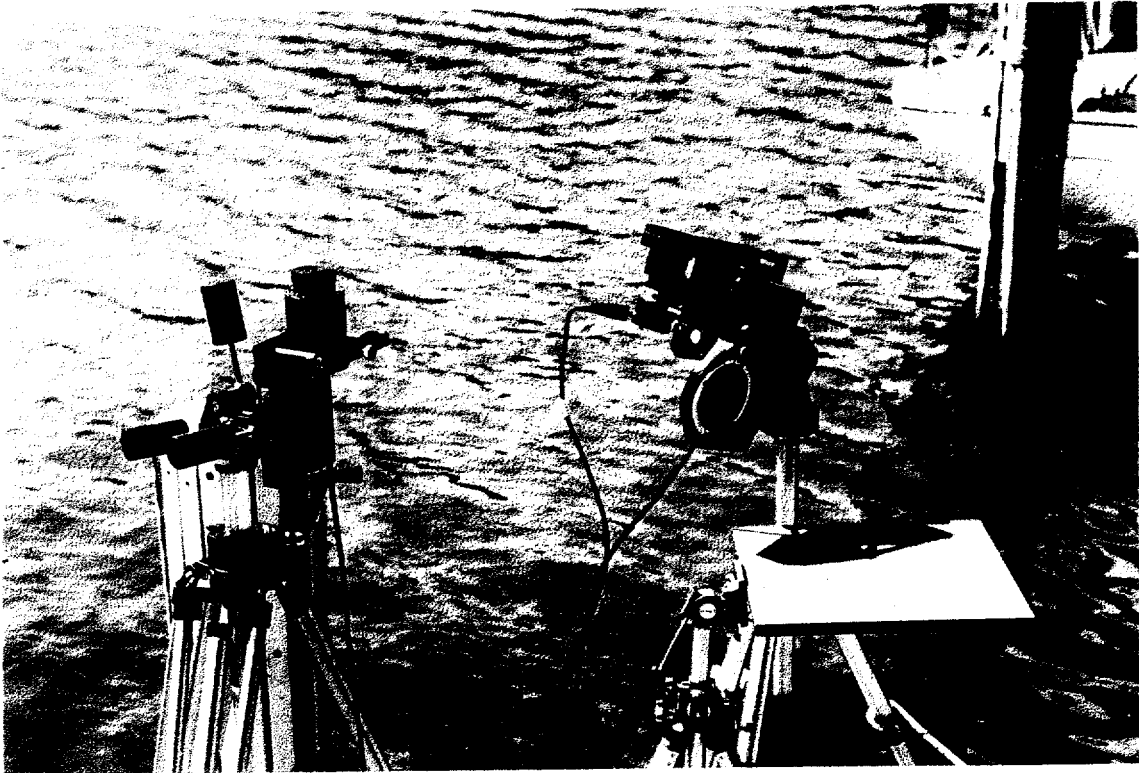


FIGURE 2.

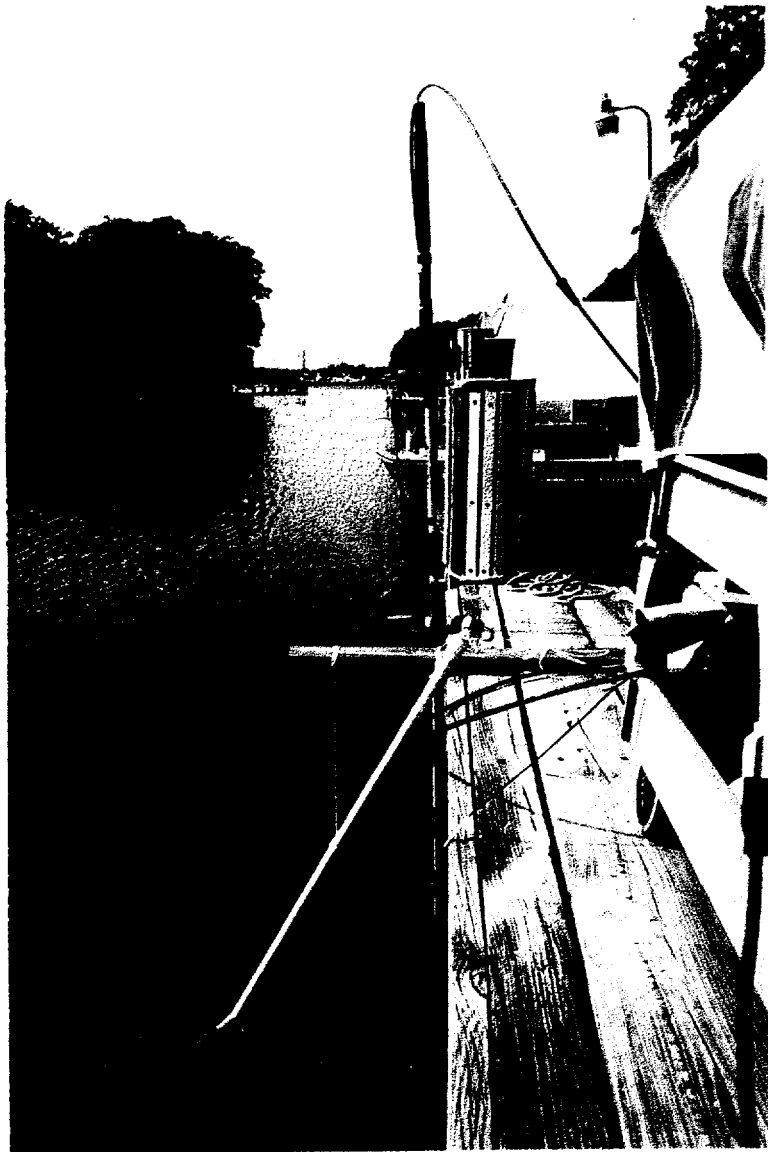


FIGURE 3

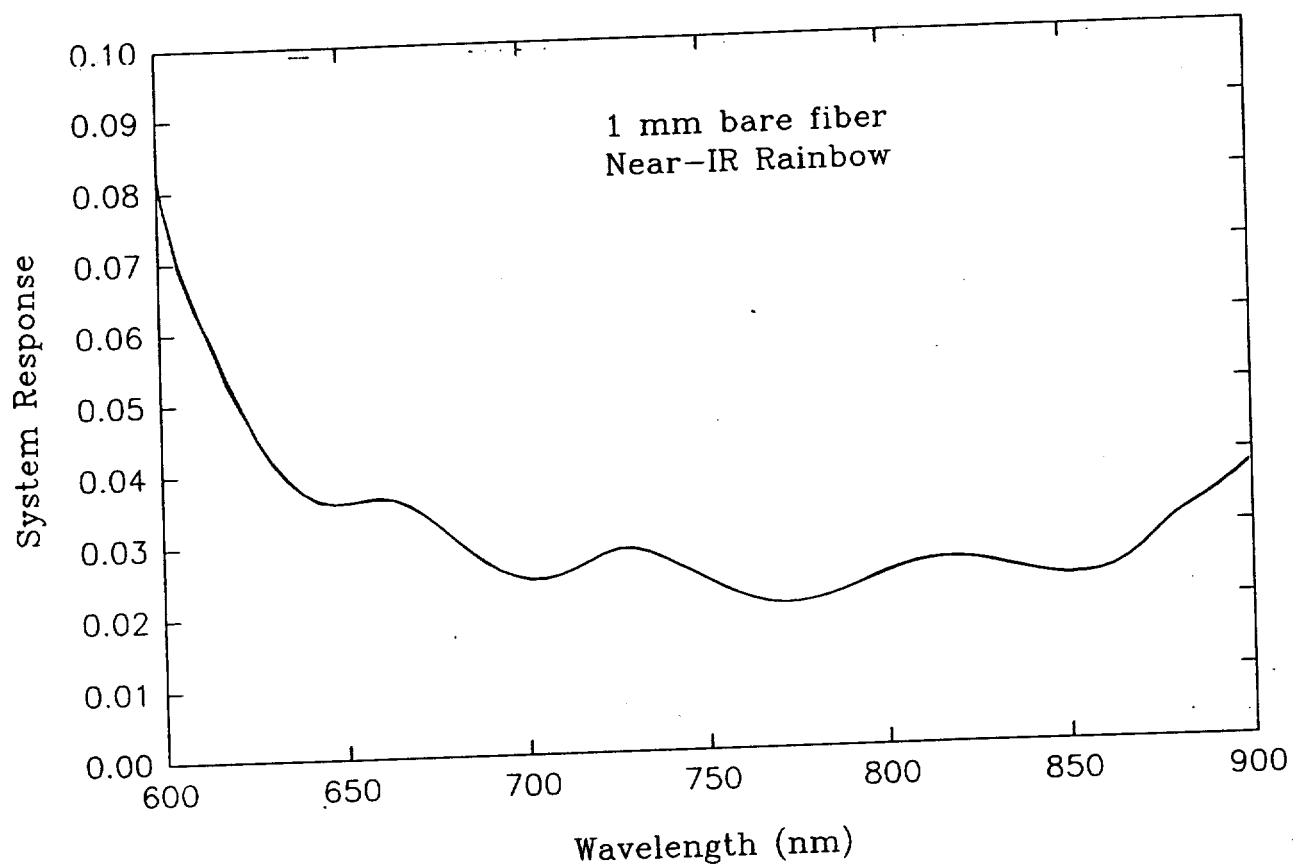


FIGURE 4.

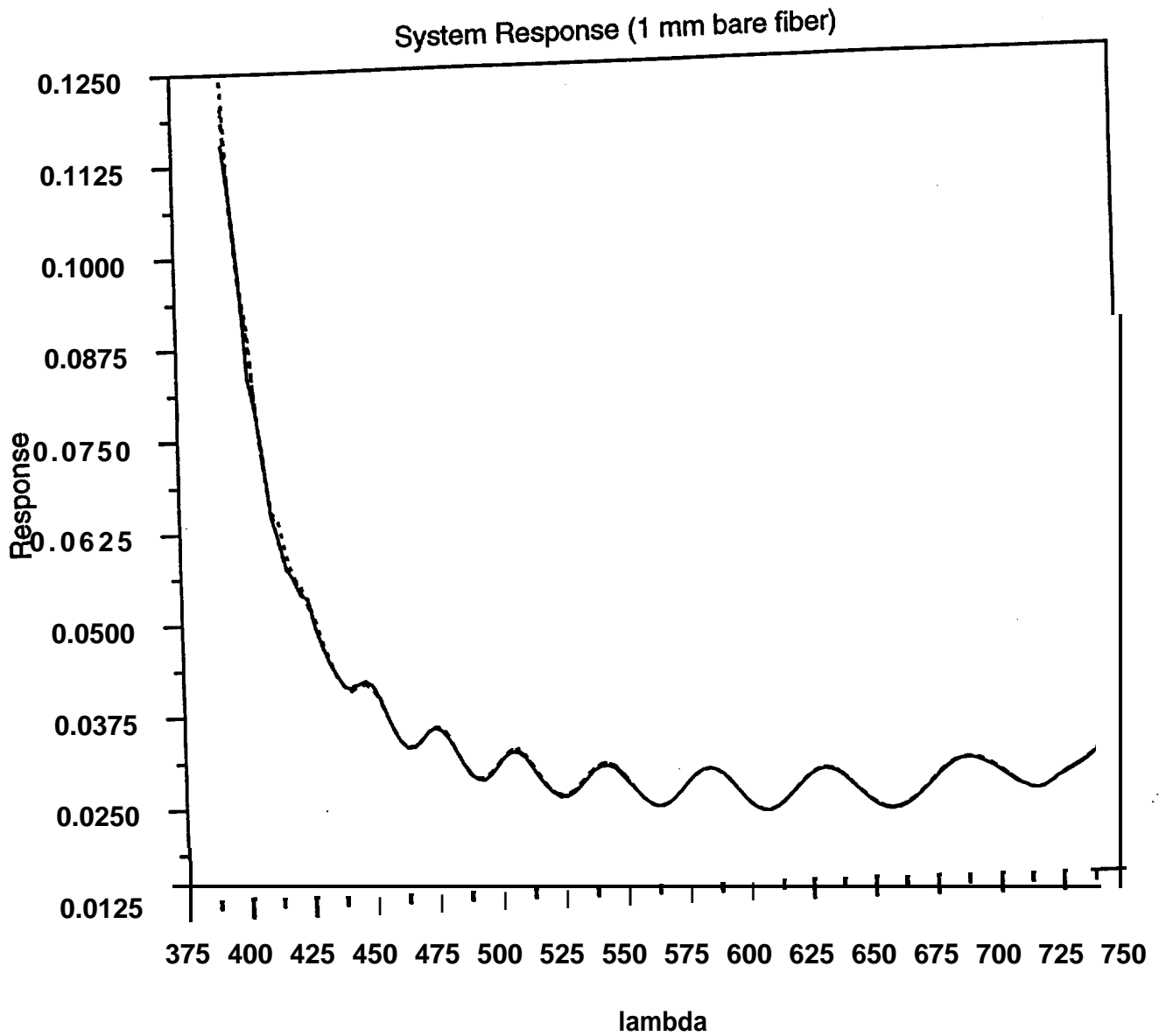


FIGURE 5.

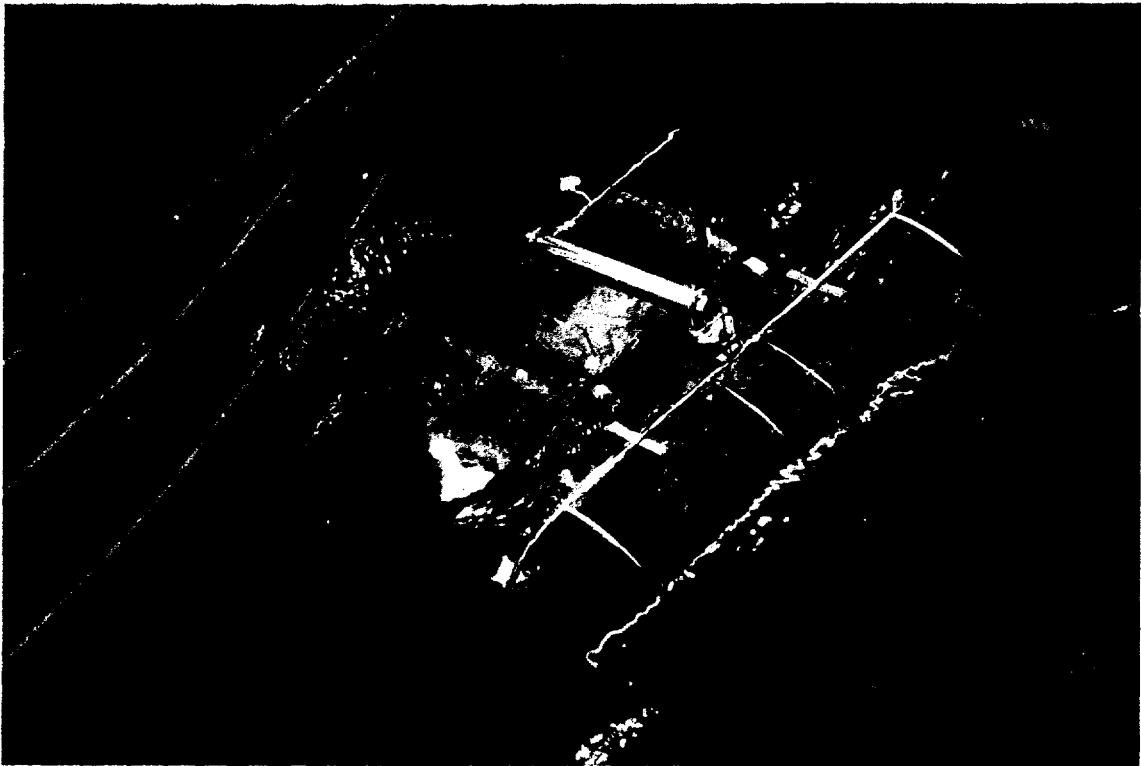
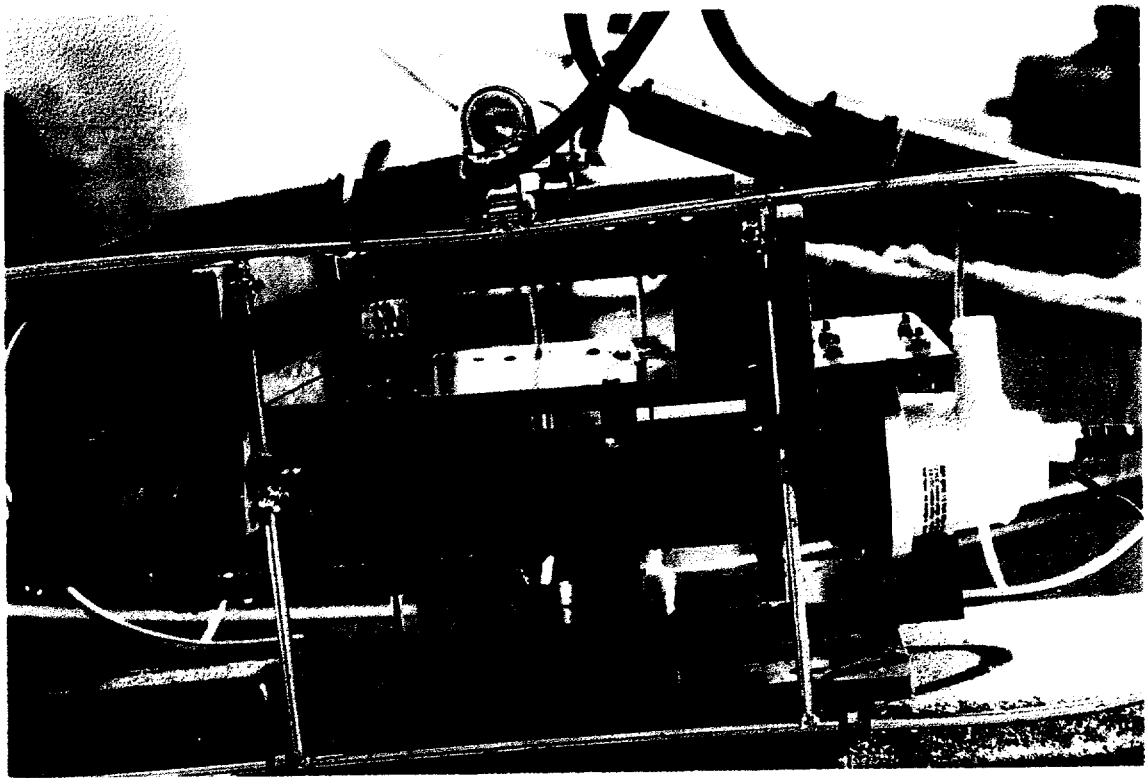


FIGURE 6

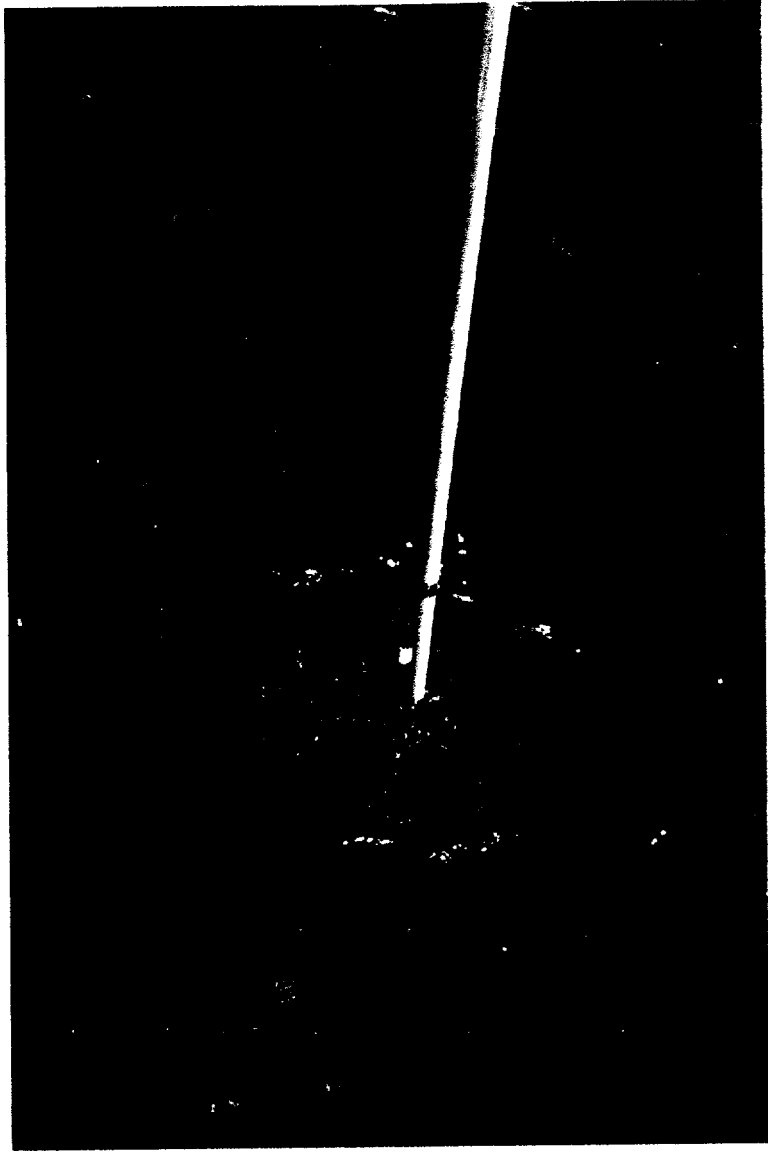


FIGURE 7.

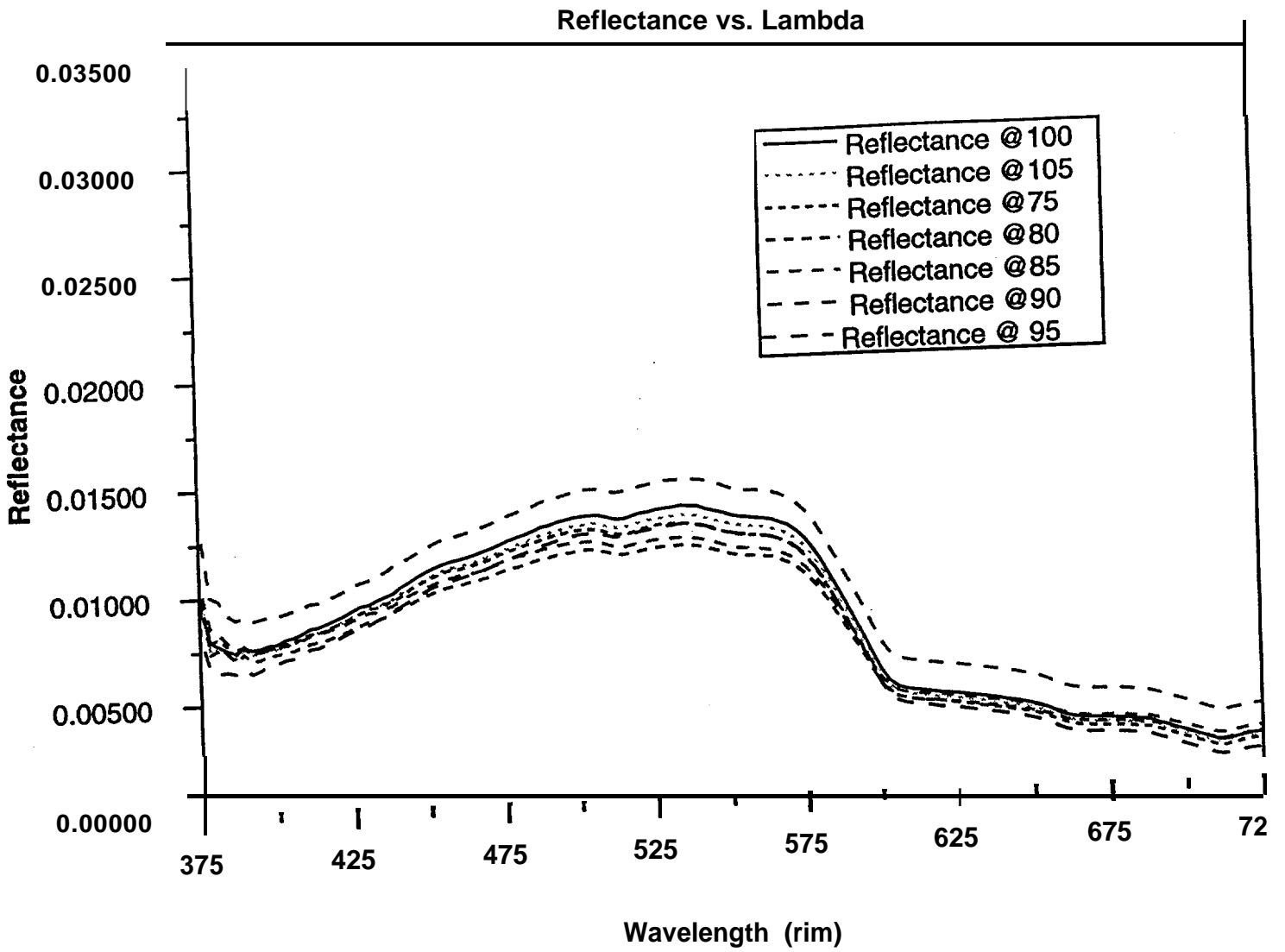


FIGURE 8.

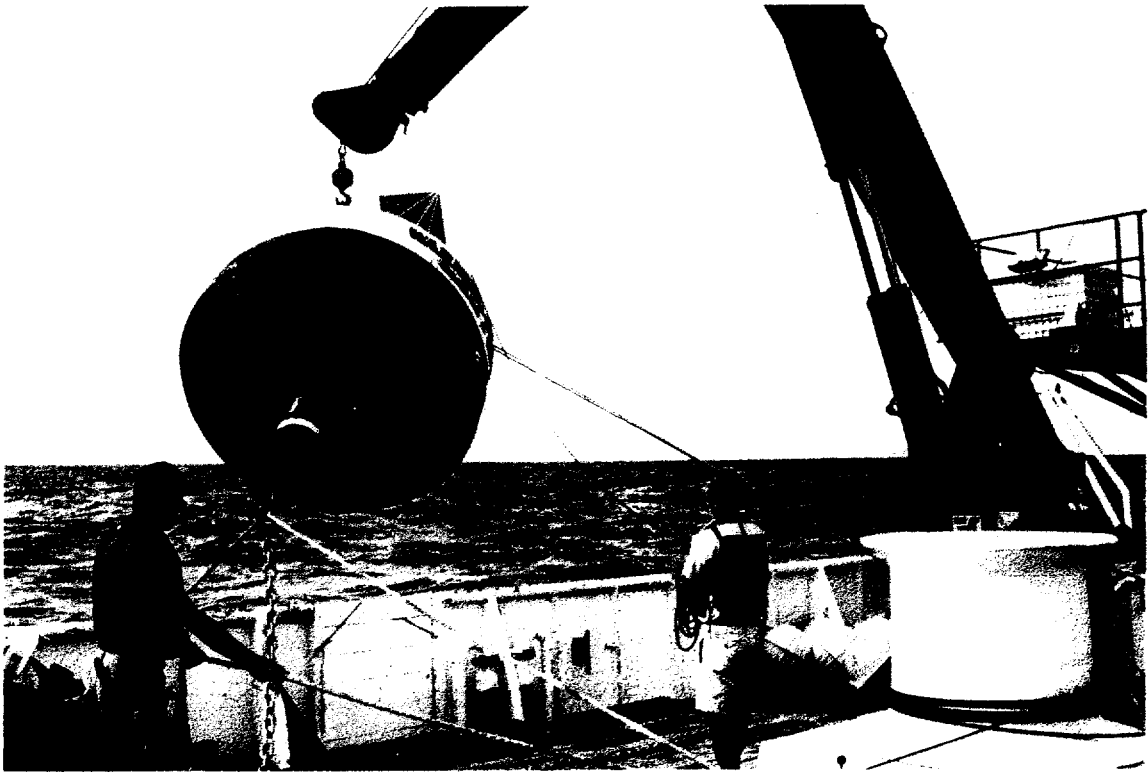
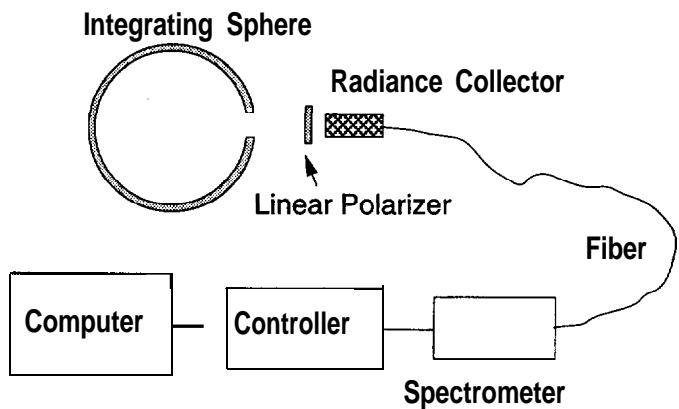


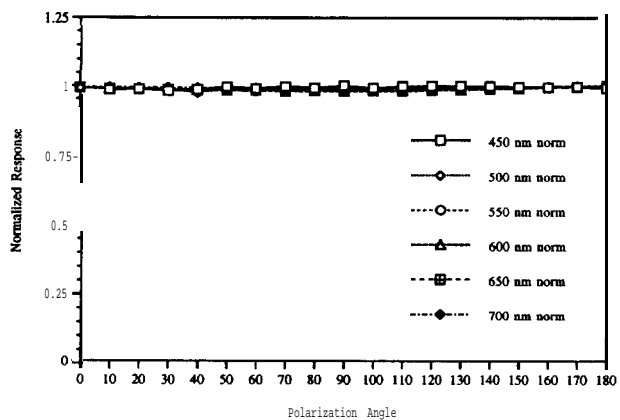
FIGURE 9.



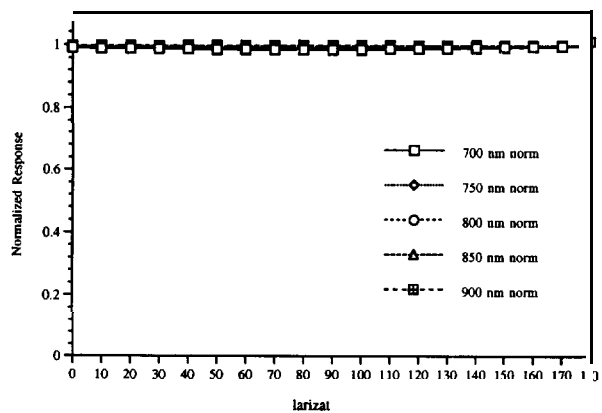
G RE



Instrument setup for polarization sensitivity characterization



Polarization sensitivity of the visible spectrometer system



Polarization sensitivity of the near-IR spectrometer system

FIGURE 11.



FIGURE 12.

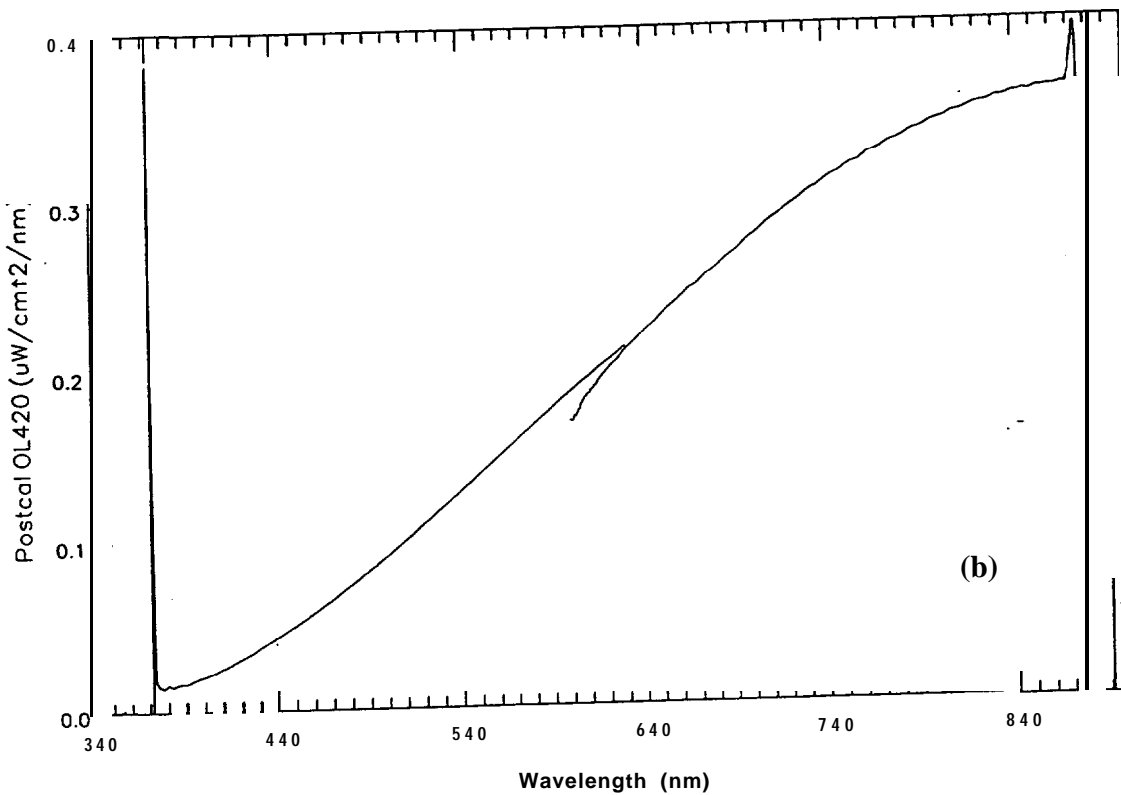
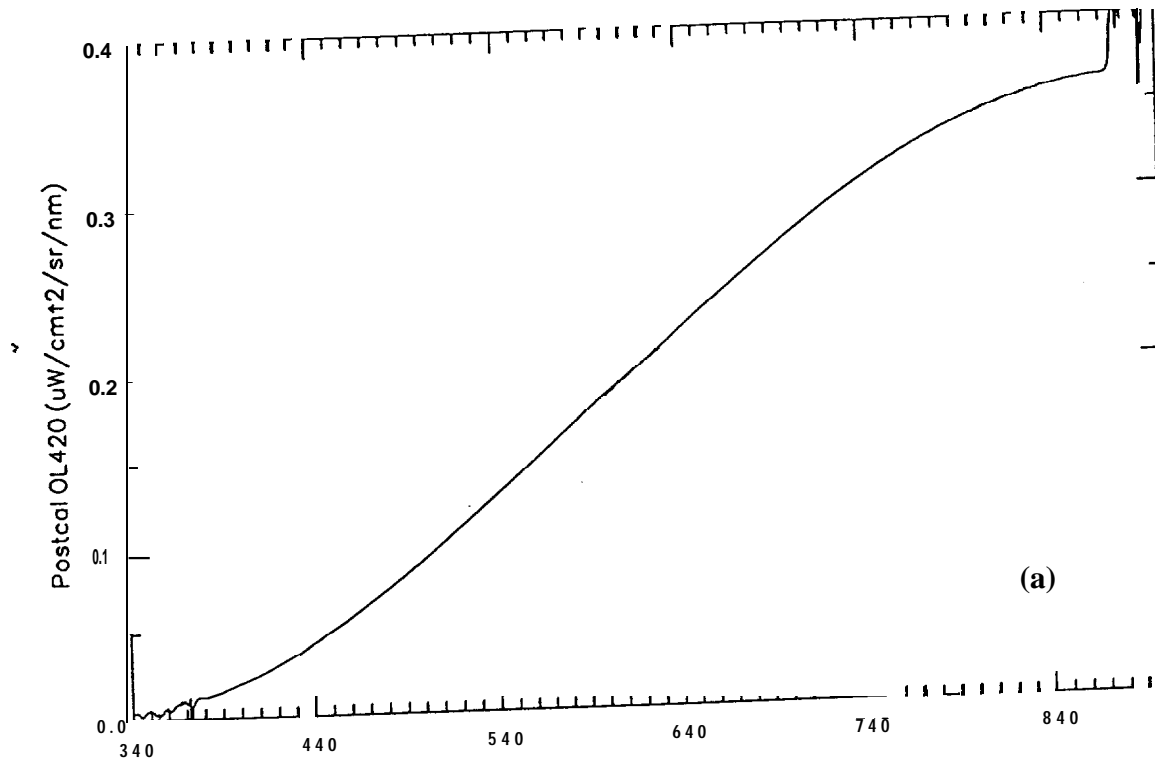


FIGURE 13. MOS Lu response derived from 1/1 sec blue/red integrations.
 (a) 1/1 sec scans converted with 1/1 sec response.
 (b) 1/0.5 sec scans converted with 1/1 sec response.

MOCE Instrumentation Software Status

Instrument	Acquisition			Processing		
	Fully Func	Mod/ Refurb	Develop & Test	Fully Func	Mod/ Refurb	Develop & Test
<i>OPTICAL</i>						
MOS 1	X			X		
MOS 2			X		X	
SIS	X			X		
MER	X			X		
Fastie	X			X		
<i>BIO OPTICAL</i>						
Transmissometer					O	X
AC-9	O					
Martek	X			X		
SeaTech	X			X		
VLST	X					X
Scattering Meter	O					
Fluorometer				X		
Chelsea	X			X		
MLML	X			X		
Turner (3)	X					X
Galai Particle Counter	X				O	
HP Spectrophotometer	X					
Microscope Video System	X			X		
Photosynthetron	X			X		
<i>ANCILLARY</i>						
Sky Camera	X					X
HHCRM	X			X		
Barometer	X			X		
Air Temperature	X			X		
% Relative Humidity	X			X		
Wind	X			X		
Compass	X					
GPS Navigation						
Trak (Time)	X			X		
Trimble (Position)	X			X		
Profiling CTDO2	X					
Alongtrack CT	X				X	O
<i>CALIBRATION</i>						
System Responses						
Irradiance	X			X		
Radiance	X			X		

X --> As of 12/94

O --> As of 8/95

TABLE 1

MOCE Instrumentation Hardware Status

Instrument	Fully Functional	Modification/ Refurbishment	Test & Evaluate
OPTICAL			
MOS 1	X		X
MOS 2			
SIS	X		
MER	X		
Fastie	X		
NO OPTICAL			
Transmissometer AC-9		O	X
Martek			O
SeaTech	X		
VLST		X	
Scattering Meter		O	X
Fluorometer			
Chelsea	X		
MLML	X		
Turner (3)	X		
Galai Particle Counter	X		
HP Spectrophotometer	X		
Microscope Video System	X		
Photosynthetron		O	
AVIONICS			
Sky Camera		X	
HHCRM		X	O
Barometer	X		
Air Temperature		O	
% Relative Humidity		O	
Wind	X		
Compass	X	O	
GPS Navigation			
Trak (Time)	O		
Trimble (Position)	X		
Profiling CTDO2	X		
Alongtrack CT	X		
Towed Paravane System		X	
CALIBRATION			
Optronix	X		
EG&G Gamma 5000	X		
Line Sources	X		
Portable Reference Lamps	X		
Diver Calibration Lamps		O	X
NIST Radiometer			O

X --> As of 12/94

O --> As of 8/95

TABLE 2

file: moce3:[mos.prc] overlap_summary.txt (rev 28Sep95 MF)

From MOCE-3 MOS Ed and Lu underwater spectra (depth = Top, Mid, Bot), examine the difference between the blue and red spectrographs in the overlap region (between -598 and 626 nm) at 609 nm. All MOS spectra were edited, smoothed, dark-adjusted and converted to radiometric units. Blue spectrum Element # 451 corresponds to 608.8 nm, red spectrum Element #520 corresponds to 608.9 nm. The blue/red overlap at 609 nm is calculated as Element# 451 minus Element# 520. Overlap is calculated from spectra without and with masked pixel offsets applied. Blue array Element# 10-30 and red array Element# 985-1000 are used for massed pixel offsets. ("*" when red counts convert to negative watts.)

Summary: The size of the blue/red overlap changed between the 'without' and the 'with' masked-pixel-offset processing the following number of times in the following 'directions':

-- SIGN CHANGE --
 INCREASE DECREASE SAME INCREASE DECREASE
 33 25 4 8 3

	#Lite Scans	B/R Int Time	Without masked pixel offsets			With masked pixel offsets		
			%Overlap Blue-Red	% 1/SNR Blue	% 1/SNR Red	%Overlap Blue-Red	% 1/SNR Blue	% 1/SNR Red
Stn 02								
Ed Top	10	0.5/0.5	- 10	14	11	- 11	14	11
Ed Mid	MISSING							
Ed Bot	5	1/16	3	12	4	3	6	2
Lu Top	5	0.25/16	4	11	2	9	18	11
Lu Mid	MISSING							
Lu Bot	5	0.5/16	7	45	31	- 0.3	7	14
Stn 03								
Ed Top	15	0.5/1	8	17	11	- 9	18	11
Ed Mid	5	0.5/4	3	4	3	- 4	4	3
Ed Bot	5	1/16	13	9	1	9	9	2
Lu Top	15	0.25/16	- 8	15	4	- 10	6	3
Lu Mid	10	0.25/16	6	15	2	8	8	2
Lu Bot	5	0.25/16	- 15	22	9	22	8	3
Stn 04								
Ed Top	5	0.5/1	- 14	9	8	- 15	9	7
Ed Mid	10	1/4	- 3	6	4	- 5	5	4
Ed Bot	5	2/16	34	45	11	- 33	12	7
Lu Top	10	0.25/16	- 10	14	4	- 17	10	4
Lu Mid	10	0.25/16	2	29	7	2	23	5
Lu Bot	5	0.5/16	64	71	17	- 10	18	8
Stn 05								
Ed Top	5	1/2	- 12	4	6	32	4	5
Ed Mid	5	2/8	2	8	8	41	7	6
Ed Bot	MISSING							
Lu Top	5	0.5/16	1	7	4	48	10	3
Lu Mid	5	0.5/16	18	20	10	50	7	5
Lu Bot	MISSING							
Stn 06								
Ed Top	5	1/2	- 10	18	19	- 11	18	19
Ed Mid	10	4/16	3	5	7	0.1	4	6
Ed Bot	10	8/16	182	50	159	- 113	6	39
Lu Top	5	0.5/16	- 14	8	12	- 20	5	12
Lu Mid	10	1/16	- 4	18	38	- 6	10	17
Lu Bot	10	2.16	- 50	85	92	- 128	20	35
Stn 08								
Ed Top	10	0.5/1	16	13	12	15	13	13
Ed Mid	10	1/8	19	29	25	18	29	25
Ed Bot	10	4/16	- 140	115	25	- 80	18	16
Lu Top	10	0.25/16	49	8	7	34	10	6
Lu Mid	10	0.5/16	39	12	4	53	11	2

TABLE 3 MOS blue/red overlap offset at 609 nm from MOCE-3.

Lu Bot	10	1/16	- 29	58	6	40	26	6
Stn 09								
Ed Top	MISSING							
Ed Mid	5	8/16	132	20	60	84	11	20
Ed Bot	5	4/16	†	1196	50	- 52	11	31
Lu Top	MISSING							
Lu Mid	5	2/16	- 13	13	20	24	13	26
Lu Bot	5	2/16	201	18	10270	55	28	20
Stn 10								
Ed Top	5	1/8	- 7	19	7	- 8	20	6
Ed Hid	5	1/8	12	14	8	13	15	5
Ed Bot	5	2/16	*	86	96	46	30	43
Lu Top	5	0.25/16	4:	42	17	23	47	16
Lu Mid	5	0.25/16	49	23	13	10	15	7
Lu Bot	5	0.5/16	95	41	16	- 11	29	7
Stn 11								
Ed Top	5	1/4	8	20	9	9	20	10
Ed Mid	10	0.5/2	- 14	11	6	- 15	10	6
Ed Bot	5	1/16	41	44	16	- 56	86	5
Lu Top	10	0.25/16	22	24	8	9	19	9
Lu Mid	10	0.25/16	30	23	7	7	17	6
Lu Bot	5	0.5/16	11	91	8	13	19	5
Stn 12								
Ed Top	5	0.5/1	1	13	9	1	13	9
Ed Mid	5	1/4	8	8	4	5	9	2
Ed Bot	5	1/16	10	5	2	9	5	2
Lu Top	10	0.25/16	19	8	9	13	7	8
Lu Mid	5	0.25/16	4	16	6	28	12	8
Lu Bot	5	0.25/16	29	42	4	19	9	5
Stn 13								
Ed Top	5	1/2	2	28	25	3	28	25
Ed Hid	5	1/4	- 16	9	10	- 17	9	9
Ed Bot	5	1/16	*	36	103	13	7	22
Lu Top	5	0.25/16	27	9	11	3	12	10
Lu Mid	5	0.25/16	26	28	5	16	22	5
Lu Bot	15	0.5/16	- 10	25	5	14	20	2
Stn 14								
Ed Top	10	2/8	2	8	5	2	8	3
Ed Mid	5	0.5/4	9	15	11	8	14	10
Ed Bot	5	1/16	3	61	18	- 29	35	12
Lu Top	10	0.5/16	23	30	11	29	30	9
Lu Mid	5	0.25/16	15	26	16	13	19	15
Lu Bot	5	0.5/16	8	42	11	- 41	65	10
Stn 15								
Ed Top	5	0.5/1	7	7	9	8	7	9
Ed Mid	5	2/8	5	4	6	4	5	6
Ed Bot	5	2/16	1	3	6	2	3	4
Lu Top	5	0.25/16	2	15	16	1	15	16
Lu Mid	10	0.5/16	14	6	3	18	5	3
Lu Bot	5	1/16	25	10	6	33	5	2
Stn 16								
Ed Top	5	0.5/1	7	26	13	8	26	12
Ed Mid	5	1/16	20	12	13	- 14	21	11
Ed Bot	5	2/16	*	34	79	235	16	96
Lu Top	10	0.25/16	18	4	3	16	7	3
Lu Mid	10	0.5/16	25	37	6	35	16	13
Lu Bot	5	1/16	19	17	46	71	24	39

Offsets applied to converted Ed and Lu scans (without masked pixel offsets) to eliminate blue/red overlap mismatch at 609 nm. Values for Ed are in $\mu\text{W}/\text{cm}^2/\text{nm}$, values for Lu are in $\mu\text{W}/\text{cm}^2/\text{sr}/\text{nm}$. Offsets were subtracted from the blue array data (Element # 1-500, -334 to 636 nm).

Stn 02	Ed Top	-7.066E+0	Stn 08	Ed Top	7.099E+0	Stn 13	Ed Top	-4.342E-1
	Ed Mid	MISSING		Ed Mid	1.271E+0		Ed Mid	-1.963E+0
	Ed Bot	3.734E-2		Ed Bot	-9.413E-2		Ed Bot	*

TABLE 3 MOS blue/red overlap offset at 609 nm from MOCE-3.

	Lu Top	6.404E-4		Lu Top	9.325E-3		Lu Top	5.118E-3
	Lu Mid	MISSING		Lu Mid	1.638E-3		Lu Mid	3.043E-3
	Lu Bot	-1.515E-4		Lu Bot	-3.901E-4		Lu Bot	-2.964E-4
Stn 03	Ed Top	-5.868E+0	Stn 09	Ed Top	MISSING	Stn 14	Ed Top	1.646E-1
	Ed Mid	-5.975E-1		Ed Mid	2.030E-1		Ed Mid	-9.182E-1
	Ed Bot	5.799E-1		Ed Bot	*		Ed Bot	2.946E-3
	Lu Top	-1.932E-3		Lu Top	MISSING		Lu Top	1.731E-3
	Lu Mid	7.053E-4		Lu Mid	-1.762E-4		Lu Mid	1.470E-3
	Lu Bot	-9.5962E-4		Lu Bot	9.033E-4		Lu Bot	1.452E-4
Stn 04	Ed Top	-1.039E+1	Stn 10	Ed Top	-7.485E-1	Stn 15	Ed Top	-2.043E+0
	Ed Mid	-4.0882E-1		Ed Mid	7.685E-1		Ed Mid	2.107E-1
	Ed Bot	4.597E-2		Ed Bot	*		Ed Bot	-1.648E-2
	Lu Top	-2.605E-3		Lu Top	6.807E-3		Lu Top	1.282E-3
	Lu Mid	1.624E-4		Lu Mid	3.814E-3		Lu Mid	2.558E-3
	Lu Bot	-1.058E-3		Lu Bot	2.315E-3		Lu Bot	1.122E-3
Stn 05	Ed Top	-3.912E+0	Stn 11	Ed Top	1.169E+0	Stn 16	Ed Top	-5.509E+0
	Ed Mid	1.266E-1		Ed Mid	-1.918E+0		Ed Mid	1.999E-3
	Ed Bot	MISSING		Ed Bot	7.612E-2		Ed Bot	*
	Lu Top	8.040E-5		Lu Top	3.144E-3		Lu Top	4.804E-3
	Lu Mid	7.105E-4		Lu Mid	2.978E-3		Lu Mid	5.940E-4
	Lu Bot	MISSING		Lu Bot	2.980E-4		Lu Bot	1.624E-4
Stn 06	Ed Top	-4.334E+0	Stn 12	Ed Top	6.820E-1			
	Ed Mid	1.002E-1		Ed Mid	1.086E+0			
	Ed Bot	3.918E-2		Ed Bot	2.906E-1			
	Lu Top	-1.025E-3		Lu Top	6.882E-3			
	Lu Mid	-8.114E-5		Lu Mid	3.419E-4			
	Lu Bot	-2.481E-4		Lu Bot	1.536E-3			

TABLE 3 MOS blue/red overlap offset at 609 nm from MOCE3.

MOCE3: [MOS.RAW] STN03_SFC_EO_01.MLDAT;1
 Offsets (BlueElmt=10-30 Red=985-1000 Dk Lt Dk VList=2,3 4-8 9,10)

Dark Blue & Red masked Element mean, RMSE,min,max,N

1405.5	27.2	1343.7	1454.1	21
3805.1	21.0	3764.0	3832.5	16

Lite Var Blue & Red Offset: mean, RMSE, min, max, N, %Offset

120.9	36.7	48.5	190.1	21	9
58.3	122.7	-98.6	307.3	21	4
-21.3	33.9	-71.7	64.9	21	-2
-14.6	39.0	-69.5	86.5	21	-1
-98.6	37.8	-162.5	0.0	21	-7
-49.6	17.6	-89.5	0.0	16	-1
-5.4	31.6	-113.5	41.5	16	-0.1
-9.1	21.2	-40.9	49.5	16	-0.2
-33.9	20.0	-77.5	3.6	16	-0.9
-108.2	17.6	-150.5	0.0	16	-3

Dark Var Blue & Red Offset: mean, RMSE, min, max, N, %Offset

-67.3	30.3	-120.7	11.3	21	-5
-44.5	16.2	-72.2	0.0	16	-1

MOCE3:[MOS.RAW]STN03_SFC_ED_02.MLDAT;1
 Offsets (BlueElmt=10-30 Red=985-1000 Dk Lt Dk Vlist=2,3 4-8 9,10)

Dark Blue & Red masked Element mean, RMSE, min, max, N

1312.7	12.8	1293.6	7337.5	21
3810.0	29.1	3764.4	3856.7	16

Lite Var Blue & Red Offset: mean, RMSE, min, max, N, %Offset

138.1	21.1	100.4	179.0	21	11
99.0	16.4	70.8	131.5	21	8
-5.4	18.9	-42.1	26.9	21	-0.4
70.6	11.4	53.5	87.3	21	5
61.6	15.4	36.2	97.4	21	5
-52.9	44.9	-198.0	28.0	16	-1
21.4	22.6	-13.0	61.9	16	0.6
77.5	29.0	-8.0	118.5	16	2
-99.8	22.3	-166.0	0.0	16	-3
51.1	25.6	-16.0	85.7	16	1

Dark Var Blue & Red Offset: mean, RMSE, min, max, N, %Offset

10.3	15.1	-16.5	34.5	21	0.8
-105.7	15.9	-136.4	0.0	16	-3

MOCE3: [MOS.RAW]STN03_SFC_ED_03.MLDAT;1
 Offsets (BlueElmt=10-30 Red=985-1000 Dk Lt Dk Vlist=2,3 4-8 9,10)

Dark Blue & Red masked Element mean, RMSE,min, max, N

1349.9	13.1	1325.2	1378.9	21
3808.6	27.7	3761.6	3875.5	16

Lite Var Blue & Red Offset: mean, RMSE, min, max, N, %Offset

105.0	72.5	1.1	209.5	21	8
67.5	18.6	37.9	99.7	21	5
-42.6	19.4	-73.8	0.0	21	-3
-33.7	20.2	-67.1	5.7	21	-3
72.2	17.6	23.3	96.1	21	5
-6.7	33.6	-92.5	89.5	16	-0.2
-101.7	25.1	-172.5	0.0	16	-3
91.4	28.5	19.5	173.5	16	2
67.1	18.2	35.5	107.5	16	2
19.3	52.0	-110.5	172.5	16	0.5

TABLE 4 MOS masked pixel offsets at Station 03 during MOCE-3.

Dark Var Blue & Red Offset: mean, RMSE, min, max, N, %Offset

1.5	14.3	-29.8	34.2	21	0.1
-11.8	18.2	-65.0	28.0	16	-0.3

MOCE3: [MOS.RAW]STN03_SFC_LU_01.MLDAT;1
 offsets (BlueElmt=10-30 Red=985-1000 Dk Lt Dk Vlist=2,3 4-8 9,10)

Dark Blue & Red masked Element mean, RMSE, min, max, N

1243.6	11.2	1220.3	1262.4	21
43827.8	369.8	43268.4	44479.0	16

Lite Var Blue & Red Offset: mean, RMSE, min, max, N, %Offset

-16.6	18.1	-49.5	23.2	21	-1
-192.7	17.6	-231.1	0.0	21	-15
-104.1	16.1	-130.3	0.0	21	-8
-106.5	15.1	-130.8	0.0	21	-9
-33.2	24.8	-88.4	0.0	21	-3
30.7	44.7	-56.6	132.0	16	0.07
-142.5	34.6	-234.0	0.0	16	-0.3
-100.5	44.6	-205.0	0.0	16	-0.2
-284.6	45.3	-407.0	0.0	16	-0.6
-81.1	41.3	-166.4	0.0	16	-0.2

Dark Var Blue & Red Offset: mean, RMSE, min, max, N, %Offset

-181.7	26.4	-243.6	0.0	21	-15
-77.8	32.2	-130.3	0.0	16	-0.2

MOCE3: [MOS.RAW]STN03_SFC_LU_02.MLDAT;1
 Offsets (BlueElmt=10-30 Red=985-1000 Dk Lt Dk Vlist=2,3 4-8 9,10)

Dark Blue & Red masked Element mean, RMSE, min,max, N

1197.9	11.7	1174.9	1221.5	21
43959.2	377.4	43334.6	44573.0	16

Lite Var Blue & Red Offset: mean, RMSE, min, max, N, %Offset

16.5	23.3	-11.7	62.9	21	1
70.4	166.4	-59.3	506.9	21	6
-67.0	17.6	-114.7	0.0	21	-6
17.2	21.1	-33.3	42.2	21	1
-165.8	12.5	-186.7	0.0	21	-14
-82.3	63.6	-195.5	46.8	16	-0.2
-60.3	14.3	-77.2	0.0	16	-0.1
-113.8	63.0	-219.7	13.8	16	-0.3
-235.0	62.2	-350.3	0.0	16	-0.5
-136.6	17.1	-191.0	0.0	16	-0.3

Dark Var Blue & Red Offset: mean, RMSE, min, max, N, %Offset

-6.0	60.4	-104.5	101.1	21	-0.5
-141.9	33.7	-200.0	0.0	16	-0.3

MOCE3: [MOS.RAW]STN03_SFC_LU_03.MLDAT;1
 Offsets (BlueElmt=10-30 Red=985-1000 Dk Lt Dk Vlist=2,3 4-8 9,10)

Dark Blue & Red masked Element mean, RMSE, min,max, N

1222.9	9.3	1206.1	1236.2	21
43945.0	362.2	43404.1	44581.5	16

Lite Var Blue & Red Offset: mean, RMSE, min, max, N, %Offset

10.2	22.9	-39.3	53.0	21	0.8
-107.5	20.0	-143.5	0.0	21	-9
-53.1	19.8	-87.0	0.0	21	-4
-228.6	87.6	-411.1	0.0	21	-19
-193.6	16.6	-219.4	0.0	21	-16

TABLE 4 MOS masked pixel offsets at Station 03 during MOCE-3.

68.8	54.0	-45.5	154.0	16	0	2
-37.0	62.6	-153.5	64.5	16	-0.08	
-44.5	55.9	-155.5	55.2	16	-0.1	
-145.4	64.8	-272.3	0.0	16	-0.3	
-211.5	18.9	-241.5	0.0	16	-0.5	

Dark Var Blue & Red Offset: mean, RMSE, min, max, N, %offset

-158.0	12.7	-189.4	0.0	21	-0.3
-163.5	37.1	-230.5	0.0	16	-0.4

MOCE3:[MOS.RAW]STN03_MID_ED_02.MLDAT;1
 Offsets (BlueElmt=10-30 Red=985-1000 Dk Lt Dk Vlist=2,3 4-8 9,10)

Dark Blue & Red masked Element mean, RMSE,min,mx,N

1477.2	9.4	1461.6	1496.2	21
12109.6	95.9	11956.2	12290.0	16

Lite Var Blue & Red Offset: mean, RMSE, min, max, N, %Offset

-35.4	24.7	-64.6	23.4	21	-2
80.3	21.4	40.4	121.4	21	5
87.2	17.7	53.8	113.9	21	6
96.9	14.9	71.3	126.5	21	7
77.8	14.7	57.9	112.0	21	5
0.6	11.3	-21.5	22.3	16	0.005
-89.4	23.1	-135.9	0.0	16	-0.7
1.0	31.7	-105.0	64.5	16	0.008
-3.4	25.4	-41.5	40.0	16	-0.03
19.0	29.6	-36.0	85.5	16	0.2

Dark Var Blue & Red Offset: mean, RMSE, min, max, N, %Offset

35.4	19.6	7.5	80.4	21	2
-50.5	25.7	-141.0	0.0	16	-0.4

MOCE3:[MOS.RAW]STN03_MID_LU_01.MLDAT;1
 Offsets (BlueElmt=10-30 Red=985-1000 Dk Lt Dk Vlist=2,3 4-8 9,10)

Dark Blue & Red masked Element mean, RMSE,min,mx, N

1161.0	10.6	1136.1	1178.1	21
43727.2	372.3	43152.2	44350.5	16

Lite Var Blue & Red Offset: mean, RMSE, min, max, N, %Offset

-54.9	18.1	-90.3	0.0	21	-5
2.2	16.7	-17.9	40.1	21	0.2
-144.8	36.7	-204.7	0.0	21	-12
-142.6	16.2	-178.5	0.0	21	-12
-17.2	18.2	-40.9	37.5	21	-1
-42.5	29.3	-88.1	26.5	16	-0.10
-264.3	37.1	-316.2	0.0	16	-0.6
-257.9	39.4	-308.8	0.0	16	-0.6
-223.7	25.5	-258.1	0.0	16	-0.5
-151.4	40.7	-246.5	0.0	16	-0.3

Dark Var Blue & Red Offset: mean, RMSE, min, max, N, %Offset

-18.6	10.4	-32.2	0.4	21	-2
-130.8	38.6	-236.0	0.0	16	-0.3

MOCE3:[MOS.RAW]STN03_MID_LU_02.MLDAT;1
 Offsets (BlueElmt=10-30 Red=985-1000 Dk Lt Dk Vlist=2,3 4-8 9,10)

Dark Blue & Red masked Element mean, RMSE, min, max, N

1126.2	13.4	1100.9	1147.8	21
43694.1	365.1	43099.1	44262.0	16

Lite Var Blue & Red Offset: mean, RMSE, min, max, N, %Offset

TABLE 4 MOS masked pixel offsets at Station 03 during MOCE-3.

-32.3	141.9	-241.8	178.3	21	-3
7.7	17.3	-19.6	40.1	21	0.7
-36.7	13.4	-51.3	0.7	21	-3
26.9	21.0	-15.6	57.1	21	2
76.9	14.2	45.6	97.8	21	7
-31.4	63.6	-132.0	82.5	16	-0.07
-159.5	71.7	-281.0	0.0	16	-0.4
-144.5	34.1	-196.0	0.0	16	-0.3
-108.7	47.0	-217.0	37.5	16	-0.2
-140.3	20.2	-165.5	0.0	16	-0.3

Dark Var Blue & Red Offset: mean, RMSE, min, max, N, %Offset

-17.7	18.5	-45.0	17.7	21	-2
-223.0	41.0	-286.0	0.0	16	-0.5

MOCE3:[MOS.RAW]STN03_BTMD01.MLDT;1
 Offsets (BlueElmt=10-30 Red=985-1000 Dk Lt Dk Vlist=2,3 4-8 9,10)

Dark Blue & Red masked Element mean, RMSE,min,max, N

2159.6	29.9	2112.4	2222.1	21
43717.7	379.4	43096.5	44361.0	16

Lite Var Blue & Red Offset: mean, RMSE, min, max, N, %Offset

12.5	15.0	-16.6	47.4	21	0.6
-35.1	15.1	-74.4	0.0	21	-2
-50.2	9.7	-73.6	0.0	21	-2
-67.8	16.0	-98.6	0.0	21	-3
-71.8	21.2	-115.3	0.0	21	-3
-19.0	51.2	-111.0	152.5	16	-0.04
-117.0	27.7	-213.0	0.0	16	-0.3
-117.1	30.6	-216.0	0.0	16	-0.3
-78.6	30.6	-185.0	0.0	16	-0.2
-28.5	46.3	-133.0	117.5	16	-0.07

Dark Var Blue & Red Offset: mean, RMSE, min, max, N, %Offset

-89.5	13.6	-114.7	0.0	21	-4
-106.1	57.9	-177.0	13.2	16	-0.2

MOCE3:[MOS.RAW]STN03_BTM_LU_01.MLDT;1
 Offsets (BlueElmt=10-30 Red=985-1000 Dk Lt Dk Vlist=2,3 4-8 9,10)

Dark Blue & Red masked Element mean, RMSE,min,max, N

1232.3	84.3	1084.0	1376.1	21
43729.5	359.7	43167.0	44333.5	16

Lite Var Blue & Red Offset: mean, RMSE, min, max, N, %Offset

-106.0	84.9	-222.1	91.2	21	-9
-161.8	86.9	-324.3	0.0	21	-13
-155.8	88.9	-310.9	0.0	21	-13
-141.9	92.2	-312.5	23.6	21	-12
-154.9	83.1	-288.3	5.4	21	-13
-20.9	54.4	-137.5	124.5	16	-0.05
-68.6	33.5	-128.4	31.5	16	-0.2
-266.2	33.5	-334.4	0.0	16	-0.6
-226.6	43.1	-292.8	0.0	16	-0.5
-289.2	33.3	-338.5	0.0	16	-0.7

Dark Var Blue & Red Offset: mean, RMSE, min, max, N, %Offset

-166.0	78.3	-303.7	0.0	21	-13
-408.9	41.0	-487.1	0.0	16	-0.9

TABLE 4 MOS masked pixel offsets at Station 03 during MOCE-3.